Relation between Surface Tension and Ion Adsorption at the Air−Water Interface: A Molecular Dynamics Simulation Study

Raffaella D'Auria and Douglas J. Tobias*

Department of Chemistry and AirUCI Environmental Molecular Sciences Institute, University of California, Irvine, Irvine, California 92697-2025

Received: November 29, 2008; Revised Manuscript Received: April 14, 2009

Classical molecular dynamics simulations of aqueous solutions of sodium chloride and potassium fluoride at two different concentrations have been carried out using polarizable force fields and standard additive force fields (not including polarizability explicitly). We show that the presence of chloride ions at the air−solution interface, as predicted from the polarizable simulations of NaCl solutions, is reconcilable with the classical thermodynamics results of Gibbs absorption theory. We discuss the role of system size in the establishment of a bulklike region in which the ion densities have converged to the same value. We compare the results for NaCl solutions with those obtained for KF at two concentrations. We find that the computed surface tension and the surface excess follow the experimental trend for each salt solution. We have characterized the extent of adsorption by calculating the fraction of the solution surface area that is occupied by each ion. The analysis reveals that, as expected, in the KF solution neither the cation nor the anion is present on the surface, regardless of whether or not a polarizable force field is employed. On the other hand, in the NaCl solutions, chloride anions occupy the surface to an extent that is roughly proportional to their bulk concentration, but only when a polarizable model is used.

Introduction

Recently, the interfacial properties of simple electrolyte solutions have received a great deal of attention.[1] The revival of this subject is largely due to two independent lines of research: unraveling the mechanism of the Hofmeister series[2] and understanding reactivity at interfaces.[1,3−14,16] The first line of research has important implications in our understanding of how biomolecules interact with each other in their solvent environment,[17] while the second is relevant to the elucidation of the mechanisms of heterogeneous atmospheric chemical processes, e.g., the formation of gas-phase chlorine from sea salt aerosols.[3]

The surface tension of inorganic salt−water solutions is generally greater than pure water,[18] and increases with salt concentration.[21,22] This effect is solute specific, with different anions having a larger influence than different cations. Anion effects on surface tension appear to follow a Hofmeister series.[19,20] For example, at a given concentration, halide anions increase the surface tension in the order: $F^- > Cl^- > Br^- > I^-$.[21,22] On the other hand, the surface tensions of alkali halide solutions are relatively insensitive to the identity of the cation (Li^+, Na^+, K^+).[19,21] Using Gibbs' thermodynamic theory of interfaces, it is possible to calculate the amount of solute adsorbed at the Gibbs dividing surface (i.e., the location, in the air−solution interfacial region, where the excess of the solvent is zero) from the activity/concentration dependence of the surface tension according to

$$\Gamma_s = -\frac{1}{RT}\left(\frac{\partial \gamma}{\partial \ln a_s}\right)_T \quad (1)$$

where R is the gas constant, T is the temperature, γ is the surface tension, and a_s is the activity of the solute, which is generally expressed as the product of the activity coefficient times the molal concentration (moles of solute/kg of solution). In the case of an ionic solution, where the solute undergoes dissociation, the activity of the solute is given by $a_s = (f^{\pm} \cdot m)^{\nu}$, where $f^{\pm}$ is the mean activity coefficient of the two dissociated ions, m is the molal concentration, and ν is the sum of the stoichiometric coefficients involved in ionic dissociation (in the case of a monovalent salt $\nu = 2$). For dilute solutions, activity coefficients are near unity, and the activity of an ion is nearly equal to its concentration. If the surface tension, γ, increases with the solute concentration, as is observed experimentally for alkali−halide aqueous solutions, its derivative will be positive and the solute surface excess, as given from eq 1, will be negative. A negative surface excess has generally been interpreted in terms of exclusion of ions from the interfacial region.[23] This interpretation was challenged recently by a series of theoretical investigations,[4−7,24,25] and experimental observations.[8−11] Consequently, it is now well established that certain ions, such as the heavier halide anions, adsorb to the air−water interface. However, the apparent contradiction between negative Gibbs surface excesses and the presence of ions at the interface has not been fully resolved.

This topic has been addressed to some extent in several recent theoretical studies. Using polarizable force fields, Jungwirth and Tobias performed molecular dynamics (MD) simulations of a series of approximately 1 M sodium halide solutions and found, consistent with experimental data, that the surface tension of the salt solutions was greater that that of neat water, and increased in the order NaI < NaBr < NaCl < NaF.[5] In the simulation of the NaF solution, both the fluoride anion and the sodium cation were repelled from the interface, as expected from the surface tension increase. However, the heavier halides were observed to adsorb to the interface with a propensity that increased in the order $Cl^- < Br^- < I^-$. While the presence of anions at the interface appears at first glance to be incompatible

* To whom correspondence should be addressed. E-mail: dtobias@uci.edu.

10.1021/jp810488p CCC: $40.75
Published on Web 05/13/2009

with the positive surface tension increments, Vrbka et al.[7] and Jungwirth and Tobias[1] proposed an explanation of how this apparent incompatibility could be resolved if the ion concentrations are characterized by oscillatory density profiles throughout the interfacial region, so that a region of ion excess is canceled out by an adjacent layer where the ions are depleted (with respect to their constant concentration level in the bulklike region). However, Jungwirth and Tobias[1] pointed out that, in their previous work, it had not been possible to obtain a quantitative description of the subsurface ion depletion due to the limited dimension of the simulation cell ($30 \times 30 \times 100$ Å^3).

Bhatt et al. addressed the issue in two papers,[26,27] with somewhat inconclusive results. In the first, they computed the surface excesses of aqueous solutions of NaCl and NaF at different concentrations using a primitive model in which the solvent is modeled as a dielectric continuum. A comparison of their computed surface excesses with experimental data was not made, but the surface tension values derived from the computed surface excesses did not agree with experimental observations, as the computed surface tension of NaCl solutions shows a larger increase with concentration than the surface tension of NaF solutions of corresponding concentrations (the opposite behavior is observed experimentally). Bhatt et al. also reported MD simulations with additive force fields (i.e., not considering polarizability) for NaF and NaCl solutions at three different concentrations. The surface tensions computed directly from the simulations agree with the trends in experimental surface tension data (note that for the NaF systems an extrapolation of the experimental data was used in the comparison because the simulations were carried out at concentrations beyond the solubility limit) but no surface excess was derived from these surface tension values. In their second study, Bhatt et al.[27] computed the surface excess of NaCl and NaBr aqueous solutions at different concentrations from MD simulations performed, once again, with additive force fields. They found that the surface excess is negative at concentrations less than roughly 4 M for NaCl, and positive at higher concentrations. For NaBr solutions, they observed an oscillatory dependence of Γ as a function of concentration. The highest concentration NaCl solution was beyond the saturation limit, and this, together with limited sampling in a short MD trajectory, may be the reason why the density profile of the system showed "pronounced peaks" reminiscent of salt crystallization. Bhatt et al.[27] noted that, in agreement with previous simulations based on polarizable models,[5,6] anion adsorption for NaCl (at 6.9 M) and NaBr (at 3.3 M) is positive.

Ishiyama and Morita[28] reported MD simulations of the solution−air interfaces of NaCl and NaI solutions at different concentrations. Their simulations were based on a flexible water model and polarizable potentials for the water and ions. In agreement with previous studies, they found an enhancement of iodide anions at the interface, followed by a subsurface depletion zone that is occupied by the counterions. However, in contrast to earlier work, chloride anions were repelled from the interface. Surface excesses computed from the density profiles for the NaCl solution were negative, in agreement with experimental data, while for the NaI solution a positive surface excess was found at the lower concentration (1.1 M) and a negative surface excess was found at the higher concentration (2.1 M). The NaCl solution results reinforce the traditional interpretation of a negative surface excess implying ion depletion from the interface, while the NaI solution results are ambiguous in this regard.

Warren and Patel[29] compared the surface excesses for 1 M solutions of NaCl, CsCl, and NaI computed from MD simulations that employed a polarizable fluctuating charge model for the water and, for the ions, either additive force fields or polarizable (Drude oscillator) ion models. With the exception of the fully polarizable NaI case, negative surface excesses were found in all cases, consistent with experiment. They also correctly reproduced the less negative excess for NaI vs NaCl solutions, and the insensitivity of the surface excess of halide solutions to the identity of the cation (e.g., Na^+ vs Cs^+). Overall, Warren and Patel obtained worse agreement with experiment when the ions were represented using the polarizable Drude oscillator vs the nonpolarizable model. They also noted that, due to pronounced oscillations in the density profiles near the interface, slabs at least 40−50 Å may be required for reliable estimates of the surface excess. Chen and Smith[30] computed the surface tension and the surface excess from MD simulations of NaCl aqueous solutions over a range of concentrations with additive force fields, and obtained very good agreement with experimental data.

It appears that, in spite of several recent investigations, a consistent connection between the macroscopic (thermodynamic) negative surface excess and the theoretically predicted and experimentally verified adsorption of ions to the interface of alkali halide solutions has not been firmly established. In addition, it is evident that calculations of surface excesses from simulations are sensitive to system size. Moreover, although it is clear that anion adsorption is enhanced by explicit treatment of electronic polarization, it is not clear that polarizable models produce better agreement with experimental values of surface tension and surface excess.

In this paper, we present results from MD simulations of aqueous solutions of two alkali halide salts, potassium fluoride and sodium chloride, at two different concentrations (approximately 1 and 6 *m*), using both polarizable and nonpolarizable potentials. In order to obtain reliable estimates of surface excesses, the slabs simulated are roughly 60 Å thick, and we have verified that this is sufficient to support a converged bulk region. Consistent with experimental data, we found that the surface tension increments of both KF and NaCl solutions increase with concentration, more so for KF vs NaCl, and we obtain negative surface excesses in all cases. Overall, the agreement with experimental data is better for the polarizable vs the nonpolarizable models. In order to quantify the adsorption of the ions at the air−solution interfaces, we computed the fraction of the solvent-accessible surface area (SASA) of the slab surfaces that is occupied by ions. We found that the SASA of sodium and potassium cations and fluoride anions is always less than 1.5% at both of the concentrations considered, regardless of the force field. The SASA analysis clearly shows that the adsorption of chloride anions is much greater when a polarizable model is used. By computing the surface tension and the surface excess, we show that the presence of chloride ions at the air−solution interface, predicted when polarizable force fields are used, is reconcilable with the classical thermodynamics results of Gibbs absorption theory.

Computational Details

Simulations of the air−soluton interface of the alkali halide aqueous solutions studied here were performed in a slab configuration[33] in which a rectangular parallelpiped-shaped simulation box containing a bulk liquid phase of the system studied is elongated in one direction (z) so that two air−liquid (or, more precisely, given the typical system sizes, two

TABLE 1: Force Field Parameters Used To Describe the Ions[a]

		nonpolarizable model		polarizable model		
	q	σ (Å)	ε (kcal/mol)	σ (Å)	ε (kcal/mol)	α (Å^3)
Na^+	+1	1.89744[b]	1.60714[b]	2.3501[d]	0.13[d]	0.24[d]
Cl^-	–1	4.41724[b]	0.11779[b]	4.3105[e]	0.10[e]	3.25[e]
K^+	+1	4.934628[c]	0.000328[c]	3.1540[f]	0.10[f]	0.83[f]
F^-	–1	2.73295[b]	0.72000[b]	3.2963[g]	0.20[g]	0.974[g]

[a] q is the charge, ε and σ are the Lennard-Jones well depth and radius, respectively, and α is the polarizability. [b] OPLS ion parameters.[40,41] [c] From Aqvist,[42] also used in the OPLS force field.[41] [d] Adapted from Smith and Dang.[43] [e] Adapted from Markovich et al.[44] [f] From Chang and Dang.[45] [g] Adapted from Perera and Berkowitz.[24]

TABLE 2: Number of Water Molecules and Ion Pairs, *n*, in Each of the Four Systems Studied[a]

	$2x2y2z$ (60 Å × 60 Å × 200 Å)		$2z$ (30 Å × 30 Å × 180 Å)	
no. of water molecules	6912		1728	
no. of ion pairs, n	144	768	30	192

[a] $2x2y2z$ systems (60 Å × 60 Å × 200 Å) were employed in the NaCl simulations and $2z$ (30 Å × 30 Å × 180 Å) systems were employed in the KF simulations.

vacuum−liquid) interfaces, perpendicular to the elongated direction, develop under the application of three-dimensional periodic boundary conditions. Molecular dynamics trajectories were run using the Amber 8 suite of programs[34] at a constant temperature of 300 K in the weak coupling ensemble.[35] The smooth particle mesh Ewald method[36] was used to compute the electrostatic interactions. The van der Waals interactions as well as the real part of the Ewald sum were truncated at 12 Å. The SHAKE algorithm[37] was used to keep the water molecules rigid. The force field parameters for the nonpolarizable and polarizable models of KF and NaCl are given in Table 1. The TIP3P water model[38] was used with the nonpolarizable ions, and the polarizable POL3 model[39] was used with the polarizable ions.

To obtain an accurate estimate of the surface excess, we have constructed slabs with a thickness of roughly 60 Å. Previous work from this group on similar systems[1] adopted a basic simulation box size of 30 Å × 30 Å × 100 Å, which contained 864 water molecules and the number of ion pairs needed to reach the desired concentration (see Figure 1). In these slabs, which we will refer to as $1z$ slabs, the typical total extent of the liquid phase between interfaces, is of 40 Å or less, depending on the concentration of the solution. The ion vertical density profiles obtained from these $1z$ slabs appeared to be not completely converged to a true bulk solution in the middle of the slab, as sustained oscillations of the ion density profiles, extending well beyond the Gibbs dividing surface, are observed. Consequently, in our previous work, it was impractical to compute certain properties, such as the surface excess of a given species, that require converged density profiles. To understand the role of the depth of the liquid phase in the establishment of a proper bulk-like region, and to compute the ion surface excess at the vapor−liquid interface of aqueous solutions of different concentrations, we have constructed two additional sets of systems (see Figure 1). The first, which will be referred to as $2z$, consists of a rectangular cell of dimensions 30 Å × 30 Å × 180 Å containing 1728 water molecules. The second, referred to as $2x2y2z$, consists of a 60 Å × 60 Å × 200 Å box containing 6912 water molecules. Both sets of systems contain the appropriate number n of ion pairs to achieve the desired

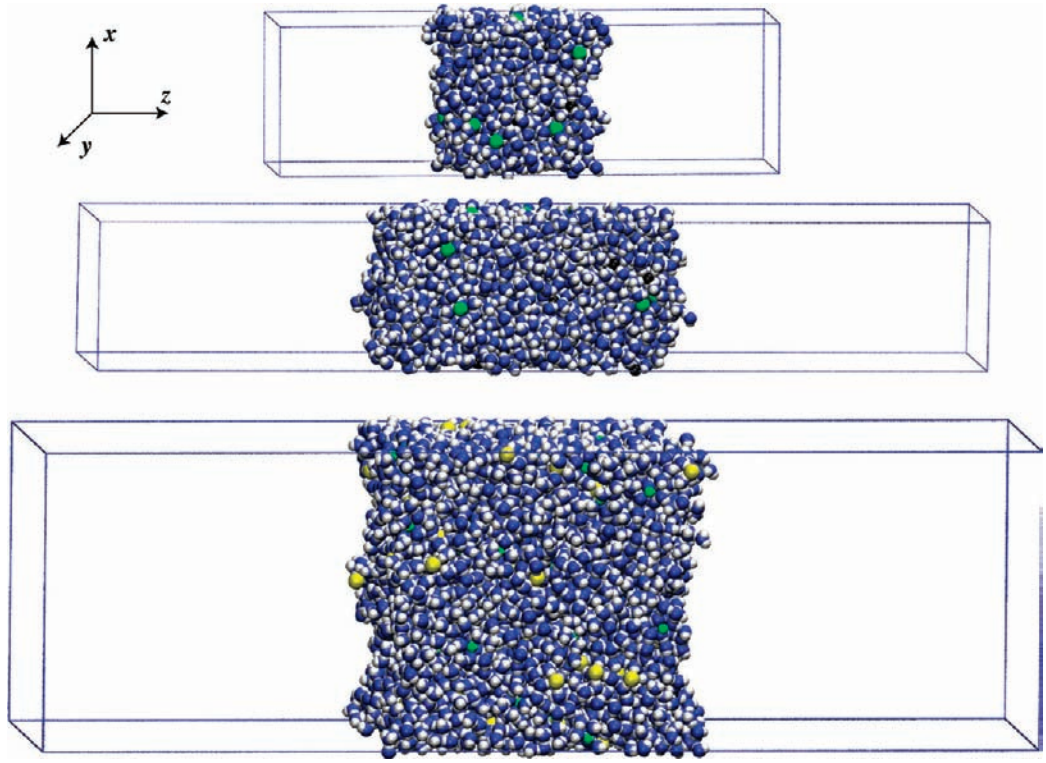

Figure 1. Top: $1z$ slab employed in previous studies[1] ($L_x \times L_y \times L_z = 30 \times 30 \times 100$ Å^3). Middle: $2z$ slab employed in this work ($L_x \times L_y \times L_z = 30 \times 30 \times 180$ Å^3). Bottom: $2x2y2z$ employed in this work ($L_x \times L_y \times L_z = 60 \times 60 \times 200$ Å^3). The top and the middle slabs shown here contain 1 m KF, and the bottom slab contains 1 m NaCl. Oxygen atoms are shown in blue, hydrogen in white, and potassium and sodium ions are in green, while fluoride ions are in black and chloride ions are in yellow.

TABLE 3: Computed (ρ_{comp}) and Experimental (ρ_{exp}) Densities for Bulk KF and NaCl Solutions at the Same Overall Concentrations of the Corresponding Slab Systems, Using Polarizable (P) and Nonpolarizable (NP) Force Fields

	KF (P)		KF (NP)		NaCl (P)		NaCl (NP)	
	0.96 m	6.17 m	0.96.m	6.17 m	1.2 m	6.17 m	1.2 m	6.17 m
ρ_{comp} (g/cm^3)	1.032	1.258	1.028	1.362	1.023	1.156	1.012	1.268
ρ_{exp} (g/cm^3)	1.042	1.247	1.042	1.259	1.041	1.189	1.040	1.191

concentrations of roughly 1 and 6 m. The results reported in this paper were obtained from 2z slabs for KF solutions and 2x2y2z slabs for NaCl solutions.

The 2z KF solutions were constructed by inserting into the middle of an equilibrated 1z system an equilibrated bulk system of roughly the same dimensions. At least 1 ns of equilibration was carried out for each of the 2z systems before data were collected for analysis. To build the 2x2y2z NaCl solutions, we first constructed 2z systems, which were equilibrated for over 5 ns, and then replicated them four times using lattice translations in the xy plane. The resulting systems were subjected to at least 1 ns of equilibration preceding the production runs.

Table 2 gives the composition of each of the systems simulated. Corresponding bulk simulations were performed in order to derive their respective densities. The bulk simulations, which were carried out at constant temperature and pressure, included 864 water molecules and an appropriate number of ion pairs to match the concentrations of the corresponding slab systems. The computed and experimental bulk densities are compared in Table 3.

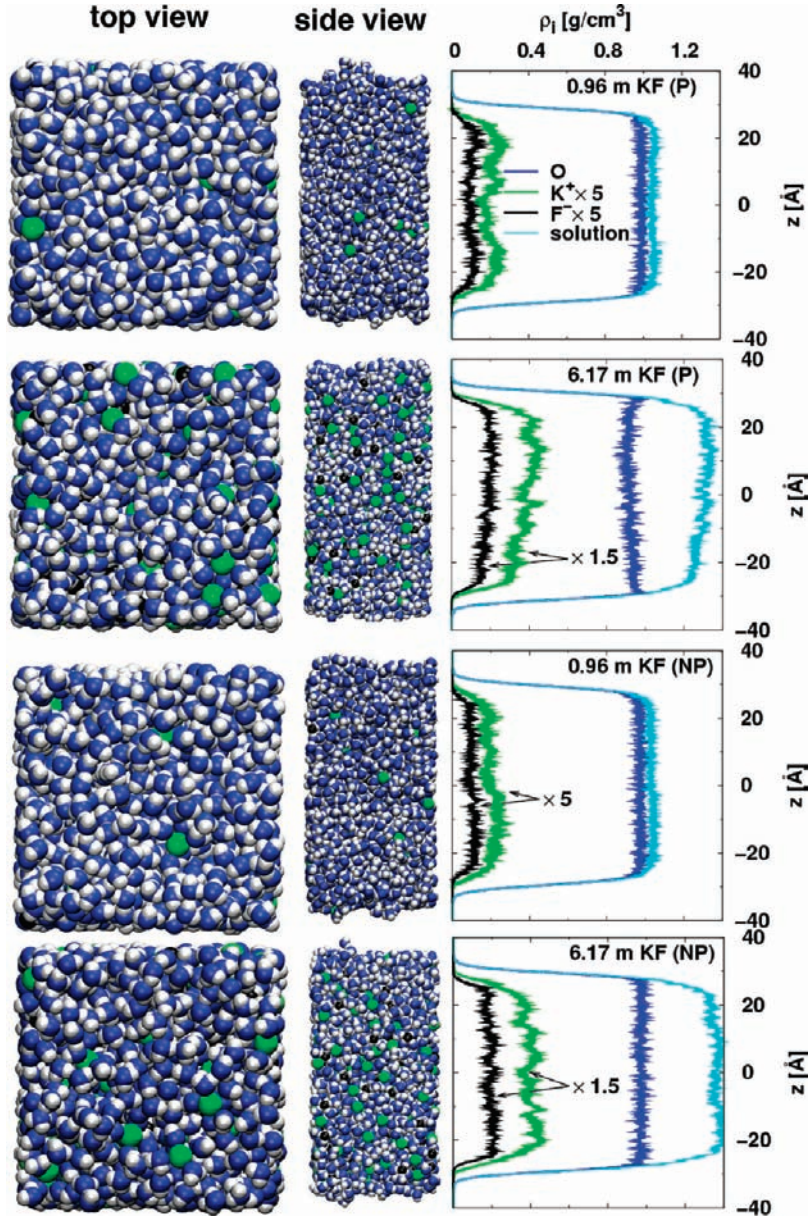

Figure 2. Top and side views of randomly chosen snapshots from the four KF systems, and density profiles of the various components (O atoms, in blue, to represent water molecules, K^+ in green and F^- in black). The solution concentration and whether a polarizable (P) or nonpolarizable (NP) force field was used is indicated in the legends of the density profile. The color of the atoms in the snapshots matches the color of the respective density profile. Hydrogens are represented in white, and the total solution density is plotted in cyan.

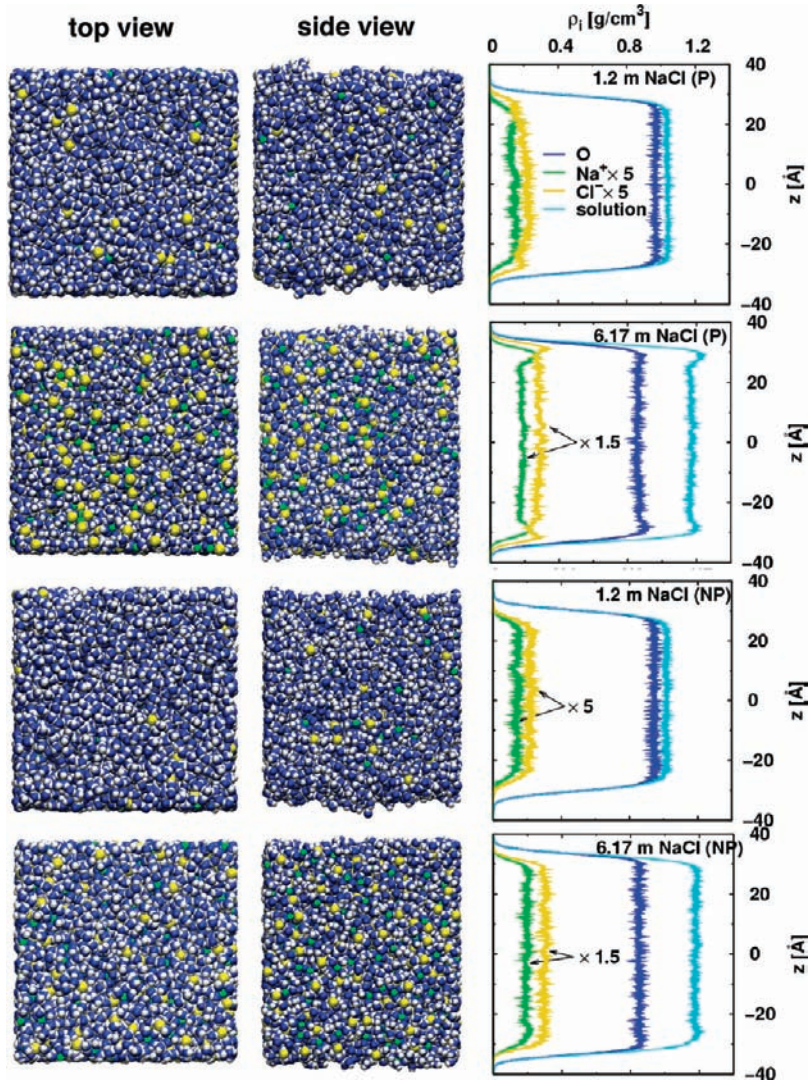

Figure 3. Top and side views of randomly chosen snapshots from the four NaCl systems, and density profiles of the various components (O atoms, in blue, to represent water molecules, Na^+ in green and Cl^- in yellow). The solution concentration and whether a polarizable (P) or nonpolarizable (NP) force field was used is indicated in the legends of the density profile. The color of the atoms in the snapshots matches the color of the respective density profile. Hydrogens are represented in white, and the total solution density is plotted in cyan.

Computation of Surface Excess, Surface Tension, and Solvent-Accessible Surface Area

In order to compute the surface excess of a given component of an aqueous solution from a molecular dynamics simulation of a system containing a liquid−vapor interface, there should be a region within the system in which the concentrations of the solute and the solvent tend to a constant, bulk value. In addition, in the case of monovalent salt solutions, the bulk concentrations of the anions and cations should be equal. Operationally, the surface excess of a solute with respect of the solvent can be written as[1]

$$\Gamma_s = \int_{-\infty}^{z_{Gibbs}} [\rho_s(z) - \rho_{sb}]\, dz + \int_{z_{Gibbs}}^{+\infty} \rho_s(z)\, dz \qquad (2)$$

where $\rho_s(z)$ is the vertical density profile of the solute and ρ_{sb} is the density of the solute in the bulk of the solution. From eq 2 it appears that one of the challenges in addressing such a problem is the need for well-converged vertical density profiles of the solute and the solvent. The convergence of solvent (water) to a constant density allows for a proper computation of the location of the Gibbs dividing surface. The latter is the idealized surface, parallel to the air−liquid interface, with respect to which the interfacial excess of a given component is computed. It is usually chosen so that the adsorption of the solvent (water) is zero, and for this reason it is also referred to as the equimolar surface. Convergence of the solute (i.e., ions) densities to a constant bulk value is also important, since at any depth below the location of the Gibbs dividing surface (z_{Gibbs}) the excess is computed by subtracting the bulk value of the density of the solute, ρ_{sb}, from its value, $\rho_s(z)$, at a position, z, in the slab. Achieving such well-converged density profiles is challenging in part because of the computational expense of extensive equilibration, and also because the size (thickness) of the slab should be large enough to permit a bulklike region to develop. In this work, we have performed MD simulations on slab systems characterized by a thicknessesof the liquid of ca. 60 Å (in the z direction).

In Figures 2 and 3 snapshots from the KF and NaCl simulations are presented along with the corresponding density profiles. The density profiles were computed as the histogram over 2 ns of trajectory following equilibration. The K^+ and F^- ions are repelled from the interface in both the polarizable and nonpolarizable cases. The NP Na^+ and Cl^- ions are similarly repelled from the interface. However, the density profiles of

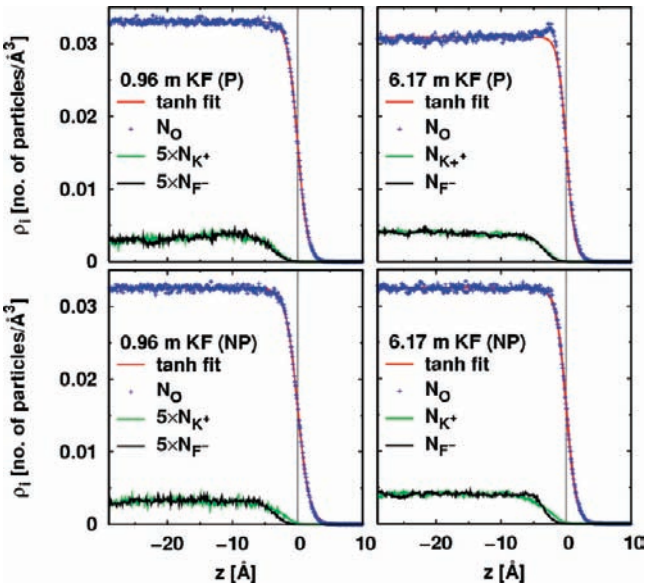

Figure 4. Symmetrized density profiles of water (O), potassium, and fluoride ions for the two polarizable and the two nonpolarizable KF solutions. The hyperbolic tangent fit to the water density profile is also shown. The z axis has been translated so that its zero corresponds to the Gibbs dividing surface (shown).

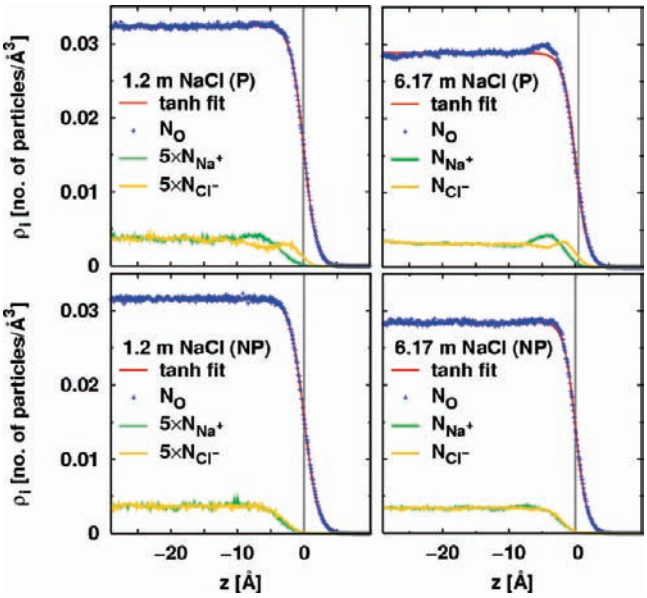

Figure 5. Symmetrized density profiles of water (O), sodium, and chloride ions for the two polarizable and the two nonpolarizable NaCl solutions. The hyperbolic tangent fit to the water density profile is also shown. The z axis has been translated so that its zero corresponds to the Gibbs dividing surface (shown). In the case of P 6.17 m NaCl solution the location of z_{Gibbs} (the height of the Gibbs dividing surface computed from direct numerical integration of the profiles, see text) is shown with respect of the zero of the figure chosen to be at z_0 (the location of the Gibbs dividing surface according to the hyperbolic tangent fit to the water density profile).

the polarizable NaCl systems show chloride ion enhancement in the interfacial region. In Figures 4 and 5 the symmetrized density profiles for all of the KF and the NaCl systems are shown. In these figures, the zero of the z axis has been placed at the Gibbs dividing surface. The latter has been obtained for each system from a fit of the symmetrized water density profile to the hyperbolic tangent function:

$$\rho(z) = \frac{1}{2}[(\rho_w^L + \rho_w^V) - (\rho_w^L + \rho_w^V)] \tanh\left(\frac{z - z_0}{\delta}\right) \quad (3)$$

where ρ_w^L is the density of water in solution (not the density of the overall solution) in the liquid phase, and ρ_w^V is the density of water in the vapor phase (which is negligible for the size of our systems), z_0 is the fitted value of the location of the Gibbs dividing surface, and δ is a parameter that describes the thickness of the water interfacial region. The latter is related to the thickness of the region in which the density of water goes from 10% to 90% of its bulk value by the simple relation $\delta_{10-90} = 2.1972\delta$. In Table 4 we report the values of these parameters, as well as the z_{Gibbs}, the position at which the water excess vanishes, computed by direct numerical integration of the symmetrized water density profiles.

In Figures 4 and 5 it is evident that the fit of the hyperbolic tangent functions to the water density profiles is overall quite good, with the exception of the polarizable ~6 m KF and NaCl systems. In the latter cases the water density profiles exhibit a peak in proximity of the air−solution interface that is not described by its hyperbolic tangent fit. Accordingly, in Table 4, we observe a corresponding discrepancy between z_0, and z_{Gibbs}.

In the case of polarizable NaCl, the chloride ions show enhancement at the interface (as a maximum in the density profiles appears), and a subsurface region in which the ion density profiles exhibit a shallow minimum, followed by a slow recovery toward the bulk value. Sodium ions show a subsurface enhancement, forming a double layer beneath the interfacial layer of chloride anions, followed by a depletion region that extends all the way down to where the chloride ion density oscillation ends. The oscillatory behavior of the ion density profiles is suppressed in the case of nonpolarizable NaCl, where both ions are mostly repelled from the interface.

The surface tension of each system was computed as the time average of the difference between the normal and the tangential components of the pressure tensor:[1]

$$\gamma = \frac{1}{2}L_z\left\langle P_{zz} - \frac{1}{2}(P_{xx} + P_{yy})\right\rangle \quad (4)$$

where L_z is the height of the box (180 Å in the $2z$ systems and 200 Å in the $2x2y2z$ systems), P_{zz} is the normal component of the pressure tensor, and P_{xx} and are the tangential components of the pressure tensor. In Table 5 we report values of the surface tension increments, $\Delta\gamma$, defined as the difference between the computed surface tensions of the solutions and that of neat water,[46] along with the corresponding surface excesses calculated from our simulations using eq 2, $\Gamma_{comp}^{+/-}$, or derived from experimental determinations of the surface tension as a function of the concentration of the solution via eq 1, Γ_{exp}.[47] Within statistical uncertainty, all of the computed surface tension increments are positive, consistent with experimental data. In addition, the computed surface tension increments for both KF and NaCl solutions increase with concentration, as expected from experiment. Overall, the surface tension increments obtained for the polarizable models are in better agreement with experiment than those obtained with the nonpolarizable models. Indeed, the polarizable models correctly reproduce the higher surface tension of a KF solution vs a NaCl solution at the same concentration, while the nonpolarizable models predict that the surface tensions of the two salt solutions are nearly equal at a given concentration.

According to the Gibbs adsorption equation (cf. eq 1), a positive surface tension increment implies a negative surface excess that should decrease (become more negative) with increasing concentration. All of the experimental and simulation

TABLE 4: Parameters Describing the Water Density Profiles for All the System Studied

	hyperbolic tangent fit				
	ρ_w^L(particles/Å^3)	z_0 (Å)	δ (Å)	δ_{10-90} (Å)	z_{Gibbs} (Å)
water[a]	0.03315 ± 0.00001	14.486 ± 0.003	1.629 ± 0.005	3.579	14.5 ± 0.1
0.96 *m* KF (P)	0.03303 ± 0.00002	29.061 ± 0.006	1.61 ± 0.01	3.54	29.0 ± 0.1
6.17 *m* KF (P)	0.03092 ± 0.00002	31.014 ± 0.007	1.30 ± 0.01	2.85	31.3 ± 0.1
0.96 *m* KF (NP)	0.03254 ± 0.00001	29.521 ± 0.004	1.807 ± 0.007	3.970	29.4 ± 0.1
6.17 *m* KF (NP)	0.03248 ± 0.00001	29.550 ± 0.004	1.534 ± 0.008	3.371	29.5 ± 0.1
1.2 *m* NaCl (P)	0.032424 ± 0.000009	29.612 ± 0.003	1.918 ± 0.006	4.215	29.6 ± 0.1
6.17 *m* NaCl (P)	0.02885 ± 0.00002	33.261 ± 0.007	1.85 ± 0.01	4.07	33.7 ± 0.1
1.2 *m* NaCl (NP)	0.03163 ± 0.000008	30.357 ± 0.003	2.111 ± 0.006	4.638	30.3 ± 0.1
6.17 *m* NaCl (NP)	0.028462 ± 0.000009	33.726 ± 0.004	1.708 ± 0.007	3.753	33.8 ± 0.1

[a] The results shown for pure water are from a standard slab containing 864 water molecules with dimensions of 30 Å × 30 Å × 100 Å. Since in the z direction this slab is half the size of the rest of the systems considered the height of z_{Gibbs} is approximately half the value of the remaining systems.

TABLE 5: Computed versus Experimental Surface Tension and Surface Excess[a]

	$\Delta\gamma_{comp}$	$\Delta\gamma_{exp}$	Γ^+_{comp}	Γ^-_{comp}	Γexp[d]
0.96 *m* KF (P)	0.6 ± 1.6	1.9[b]	−0.05	−0.04	−0.2
6.17 *m* KF (P)	13.8 ± 3.0	12.1[b]	−2.0	−2.0	−0.6
0.96 *m* KF (NP)	4.7 ± 2.7	1.9[b]	−0.2	−0.2	−0.2
6.17 *m* KF (NP)	18.3 ± 4.7	12.1[b]	−1.3	−1.3	−0.6
1.2 *m* NaCl (P)	−0.9 ± 1.3	1.6[c]	−0.2	−0.2	−0.2
6.17 *m* NaCl (P)	4.3 ± 1.9	8.2[c]	−0.6	−0.6	−0.6
1.2 *m* NaCl (NP)	5.4 ± 3.4	1.6[c]	− 0.3	− 0.3	− 0.2
6.17 *m* NaCl (NP)	16.0 ± 4.9	8.2[c]	− 0.8	− 0.8	− 0.6

[a] Errors, when present, have been computed using the method of blocking transformations.[32] [b] Data from the International Critical Tables.[21] [c] From Hård and Johansson.[22] [d] Surface excess values computed from the activity dependence of experimental surface tension data.[47] Note that the values reported are for the individual ions, and hence are half the values for the salts.

TABLE 6: Computed Solvent-Accessible Surface Areas (SASA)[a]

	%SASA$^+$	%SASA$^-$
0.96 *m* KF (P)	0.11 ± 0.03	0.06 ± 0.03
6.17 *m* KF (P)	0.54 ± 0.10	0.17 ± 0.04
0.96 *m* KF (NP)	0.33 ± 0.06	0.05 ± 0.01
6.17 *m* KF (NP)	1.35 ± 0.17	0.32 ± 0.05
1.2 *m* NaCl (P)	0.10 ± 0.02	1.66 ± 0.10
6.17 *m* NaCl (P)	1.38 ± 0.08	13.23 ± 0.61
1.2 *m* NaCl (NP)	0.007 ± 0.003	0.065 ± 0.016
6.17 *m* NaCl (NP)	0.66 ± 0.09	1.41 ± 0.08

[a] Errors have been computed using the method of blocking transformations.[32]

values of the surface excess in Table 5 are consistent with these expectations from thermodynamics. Although both the polarizable and nonpolarizable models for KF and NaCl exhibit excellent qualitative agreement with surface excesses extracted from the concentration dependence of experimental surface tension data, the quantitative agreement appears to be better for the results obtained with the nonpolarizable KF and the polarizable NaCl. In the case of KF, the better agreement with experimental surface tension for the polarizable model and surface excess for the nonpolarizable appears to be contradictory based on eq 1. Strictly speaking, if we used eq 1 to calculate the surface excess from simulation data on the activity dependence of computed surface tensions, we would expect one of the models (polarizable or nonpolarizable) to consistently show better agreement with both the surface tension increment and the corresponding surface excess. However, we used eqs 4 and 2 to calculate surface tension and surface excess, respectively, from the simulations. Thus, in light of the considerable statistical uncertainties in each of the quantities, consistent compatibility with experimental thermodynamic data is not guaranteed.

The traditional interpretation of the positive surface tension increments and corresponding negative surface excesses of aqueous solutions of simple inorganic ions has been that the ions are repelled or depleted from the air−solution interface.[1] The density profiles plotted in Figures 3 and 5 for NaCl suggests a substantial population of chloride anions at the interface when a polarizable model is used. Thus, the simulations of NaCl solutions based on polarizable force fields show that the presence of ions at the interface is reconcilable with negative surface excesses if the ion density profiles are oscillatory, as suggested previously.[1]

The top-view snapshots from the simulations depicted in Figures 2 and 3 suggest that there are some ions present on the surface of all of the solutions considered, although chloride anions are much more prevalent on the surface than the cations and fluoride anions. Moreover, it is clear that the adsorption of chloride is substantially greater when a polarizable model is employed. To quantify presence the of ions on the surface of the solutions, we have calculated their solvent-accessible surface areas (SASA) using an algorithm implemented in the VMD molecular graphics and trajectory analysis program.[48] The probe radius was chosen to be 1.7 Å, which is roughly representative of a water molecule or hydroxyl radical, the latter being of interest because of the reactivity of halide anions to OH in heterogeneous atmospheric processes.[3] In Table 6 we express the results as the percentage of the air−solution interface, %SASA$^+$ and %SASA$^-$, occupied by the cations and anions, respectively. The results show that the population of ions on the surface of the solutions is very small (<1.5%) in all of the systems except for the 6 *m* NaCl solution, for which, consistent with previous simulations of a similar system,[3,4] chloride anions occupy ≈12% of the total surface area.

Conclusions

Molecular dynamics simulations have been used to explore the relation between surface tension increments, Gibbs surface excesses, and the adsorption of ions at the air−solution interface. For simple inorganic electrolytes such as the alkali halides, it is well established experimentally that the surface tensions of the solutions increase, and the surface excesses therefore become more negative, as the salt concentration is increased. Our MD simulations of KF and NaCl solutions at 1 and 6 *m* concentrations qualitatively reproduced the experimental trends, regardless of whether or not a polarizable or nonpolarizable force field was used to describe the ions and water molecules. Calculation of the extent of surface coverage by ions via solvent-accessible surface areas revealed that the hard alkali cations and fluoride anions are essentially absent from the surface of the solutions modeled with either polarizable or nonpolarizable potentials,

and that chloride anions do not strongly adsorb to the interface when described by a nonpolarizable potential. On the other hand, chloride anions adsorb to the surface with a population that is roughly proportional to concentration when a polarizable model is employed. Calculation of the Gibbs surface excesses by integration of ion density profiles explicitly confirmed our previous suggestion[1] that the presence of ions at the air−solution interface is compatible with negative surface excesses when the ion density profiles are oscillatory, and the subsurface depletion compensates for the surface enhancement of the adsorbing ion, as was observed in the present study for polarizable NaCl. The main objective of the present investigation was to demonstrate that ion adsorption to the air−water interface, as reported here for a polarizable model of chloride anion, is not incompatible with positive surface tension increments and corresponding negative surface excesses.

The results of the present investigation clearly show that the extent of adsorption of polarizable anions (such as chloride) to the air−water interface, as predicted by molecular simulations, depends sensitively on whether or not electronic polarization is explicitly accounted for in the force field employed. Several previous simulation studies have noted the importance of including both ion and water polarization in the extent of ion adsorption to the air−water interface predicted by molecular simulation.[1,7] A theory of polarizable ions, which clearly demonstrates that ion polarization drives ion adsorption at aqueous interfaces, was published recently.[49] The role of ion size in promoting adsorption to the air−water interfaces has also been recognized.[1,7] Although it is widely acknowledged that both ion size and polarizability play a role in interfacial adsorption, the relative importance of the two effects depends on the details of the force field models employed. The results of the present investigation indicate that comparison of theoretically predicted and experimentally measured interfacial thermodynamic quantities, such as surface tension and surface excess, might not be sufficient for quantitatively assessing the relative roles of ion properties in determining their interfacial propensities.

Acknowledgment. This work has been supported by the AirUCI Environmental Molecular Sciences Institute under grant CHE-0431512 from the National Science Foundation. We are grateful to Prof. John Wheeler at UCSD for helpful discussions concerning the calculation of Gibbs surface excesses from MD simulation data.

References and Notes

(1) Jungwirth, P.; Tobias, D. J. *Chem. Rev.* **2006**, *106*, 1259–1281.
(2) Tobias, D. J.; Hemminger, J. C. *Science* **2008**, *319*, 1197–1198.
(3) Knipping, E. M.; Lakin, M. J.; Foster, K. L.; Jungwirth, P.; Tobias, D. J.; Gerber, R. B.; Dabdub, D.; Finlayson-Pitts, B. J. *Science* **2000**, *288*, 301–306.
(4) Jungwirth, P.; Tobias, D. J. *J. Phys. Chem. B* **2000**, *104*, 7702–7706.
(5) Jungwirth, P.; Tobias, D. J. *J. Phys. Chem. B* **2001**, *105*, 10468–10472.
(6) Jungwirth, P.; Tobias, D. J. *J. Phys. Chem. B* **2002**, *106*, 6361–6376.
(7) Vrbka, L.; Mucha, M.; Minofar, B.; Jungwirth, P.; Brown, E. C.; Tobias, D. J. *Curr. Opin. Colloid Interface Sci.* **2004**, *9*, 67–73.
(8) Winter, B.; Weber, R.; Schmidt, P. M.; Hertel, I. V.; Faubel, M.; Vrbka, L.; Jungwirth, P. *J. Phys. Chem. B.* **2004**, *108*, 14558–14564.
(9) Weber, R.; Winter, B.; Schmidt, P. M.; Widdra, W.; Hertel, I. V.; Dittmar, M.; Faubel, M. *J. Phys. Chem. B,* **2004**, *108*, 4729–4736.
(10) Petersen, P. B.; Saykally, R. J. *Chem. Phys. Lett.* **2004**, *397*, 51–55.
(11) Liu, D. F.; Ma, G.; Levering, L. M.; Allen, H. C. *J. Phys. Chem. B* **2004**, *108*, 2252–2260.
(12) Raymond, E. A.; Richmond, G. L. *J. Phys. Chem. B* **2004**, *108*, 5051–5059.
(13) Andersson, G.; Krebs, T.; Morgner, H. *Phys. Chem. Chem. Phys.* **2005**, *7*, 2948–2954.
(14) Ghosal, S.; Hemminger, J. C.; Bluhm, H.; Mun, B. S.; Hebenstreit, E. E. D.; Ketteker, G.; Ogletree, D. F.; Requjo, F. G.; Salmeron, M. *Science* **2005**, *307*, 563–566.
(15) Jungwirth, P.; Tobias, D. J. *Chem. Rev.* **2006**, *106*, 1259–1281.
(16) Brown, M. A.; D'Auria, R.; Kuo, I.-F. W.; Krisch, M. J.; Starr, D. E.; Bluhm, H.; Tobias, D. J.; Hemminger, J. C. *Phys. Chem. Chem. Phys.* **2008**, *10*, 4778–4784.
(17) Zhang, Y.; Cremer, P. S. *Curr. Opin. Chem. Biol.* **2006**, *10*, 658–663.
(18) Heydweiller, A. *Ann. Phys.* **1910**, *33*, 145.
(19) Jarvis, N. L.; Scheiman, M. A. *J. Phys. Chem.* **1968**, *72*, 74–78.
(20) Pegram, L. M.; Record, M. T., Jr. *J. Phys. Chem. B,* **2007**, *111*, 5411–5417.
(21) Washburn, E. W. *International Critical Tables of Numerical Data. Physics, Chemistry, and Technology*; McGraw-Hill: New York, 1928; Vol. IV.
(22) Härd, S.; Johansson, K. *J. Col. Int. Sci.* **1977**, *60*, 467–472.
(23) Adam, N. K. *The Physics and Chemistry of Surfaces*; Oxford University Press: London, 1941.
(24) Perera, L.; Berkowitz, M. L. *J. Chem. Phys.* **1994**, *100*, 3085–3093.
(25) Dang, L. W.; Rice, J. E.; Caldwell, J.; Kollman, P. A. *J. Am. Chem. Soc.* **1991**, *113*, 2481–2486.
(26) Bhatt, D.; Newman, J.; Radke, C. J. *J. Phys. Chem. B* **2004**, *108*, 9077–9084.
(27) Bhatt, D.; Chee, R.; Newman, J.; Radke, C. J. *Curr. Opin. Colloid Interface Sci.* **2004**, *9*, 145–148.
(28) Ishiyama, T.; Morita, A. *J. Phys. Chem. C* **2006**, *111*, 721–737.
(29) Warren, G. L.; Patel, S. *J. Phys. Chem. C* **2008**, *112*, 7455–7467.
(30) Chen, F.; Smith, P. E. *J. Phys. Chem. B* **2008**, *112*, 8975–8984.
(31) Söhnel, O.; Novotný, P. *Densities of Aqueous Solutions of Inorganic Substances*; Elsevier: New York, 1985.
(32) Flyvbjerg, H.; Petersen, H. G. *J. Chem. Phys.* **1898**, *91*, 461–466.
(33) Benjamin, I. *J. Chem. Phys.* **1991**, *95*, 3698–3709.
(34) Case, D. A.; Darden, T. A.; Cheatham, T. E., III.; Simmerling, C. L.; Wang, J.; Duke, R. E.; Luo, R.; Merz, K. M.; Wang, B.; Pearlman, D. A.; Crowley, M.; Brozell, S.; Tsui, V.; Gohlke, H.; Mongan, J.; Hornak, V.; Cui, G.; Beroza, P.; Schafmeister, C.; Caldwell, J. W.; Ross, W. S.; Kollman, P. A. *AMBER 8*; University of California: San Francisco, 2004.
(35) Berendsen, H. J. C.; Postma, J. P. M.; Vangunsteren, W. F.; Dinola, A.; Haak, J. R. *J. Chem. Phys.* **1984**, *81*, 3684–3690.
(36) Essmann, U.; Perera, L.; Berkowitz, M. L.; Darden, T.; Lee, H.; Pedersen, L. G. *J. Chem. Phys.* **1995**, *103*, 8577–8593.
(37) Ryckaert, J.-P.; Ciccotti, G.; Berendsen, H. J. C. *J. Comput. Phys.* **1977**, *23*, 327–341.
(38) Jorgensen, W. L.; Chandrasekhar, J.; Madura, J.; Klein, M. L. *J. Chem. Phys.* **1983**, *79*, 926–935.
(39) Caldwell, J. W.; Kollman, P. A. *J. Phys. Chem.* **1995**, *99*, 6208–6219.
(40) Chandrasekhar, J.; Spellmeyer, D. C.; Jorgensen, W. L. *J. Am. Chem. Soc.* **1984**, *106*, 903–910.
(41) Jorgensen, W. L."OPLS all-atom parameters for organic molecules, ions, and nucleic acids", available by sending an e-mail to W. L. Jorgensen.
(42) Åqvist, J. *J. Phys. Chem.* **1990**, *94*, 8021–8024.
(43) Smith, D. E.; Dang, L. X. *J. Chem. Phys.* **1994**, *100*, 3757–3765.
(44) Markovich, G.; Perera, L.; Berkowitz, M. L.; Cheshnovsky, O. *J. Chem. Phys.* **1996**, *105*, 2675–2684.
(45) Chang, T.-M.; Dang, L. X. *J. Phys. Chem. B,* **1999**, *103*, 4717–4720.
(46) Note that the surface tension for neat water was computed from a 1z slab containing only water. POL3 water was used to compute the reference water surface tension for the polarizable simulations, while TIP3P water was used to compute the reference surface tension of water for the non polarizable systems.
(47) Note that, experimentally, the surface tension is usually measured as a function of the molality of the solution, and not of its activity. The relation between the molality, m, and activity, a, is given by $a = fm$, where f, the activity coefficients, are a function of the molal concentration. To compute Γ_{exp} from the experimental surface tension data, we have to recast the latter as a function of the activity rather then the molality of the solution. In this work we have used the activity coefficients for KF from: Lide, D. R., Ed.; *CRC Handbook of Physics and Chemistry*, 87th ed.; Internet version, 2007; and for NaCl as compiled by: Gazith, M. *Activity coefficients of various electrolytes. Molal and molar concentrations*; Atomic Energy Commission, Soreq Research Establishment: Rehovoth, Israel, 1964. We have computed $(\partial\gamma/\partial a)_T$ from the analytical derivative of a function fitted to the experimental surface tension data of KF[22] and of NaCl,[21] where these data, originally given as a function of molality, were expressed as a function of the activity of the solution.
(48) Humphrey, W.; Dalke, A.; Schulten, K. *J. Mol. Graphics* **1996**, *14*, 33–38.
(49) Levin, Y. *Phys. Rev. Lett.* **2009**, *102*, 147803.

JP810488P